

Optical switching and related structural properties of epitaxial $\text{Ge}_2\text{Sb}_2\text{Te}_5$ films

F. Gericke, T. Flissikowski,^{a)} J. Lähnemann, F. Katmis, W. Braun,^{b)} H. Riechert, and H. T. Grahn

Paul-Drude-Institut für Festkörperelektronik, Hausvogteiplatz 5–7, 10117 Berlin, Germany

(Received 9 March 2012; accepted 9 May 2012; published online 11 June 2012)

We investigate the optical switching process and the related structural properties of $(\text{GeTe})(\text{Sb}_2\text{Te}_3)$ epitaxial films close to $\text{Ge}_2\text{Sb}_2\text{Te}_5$ composition on $\text{GaSb}(001)$. While the amorphization process can take place in a single or in multiple steps, the re-crystallization process always takes place in multiple steps. Intermediate stages of the re-crystallization process are characterized by small crystalline islands within the amorphous area. The structural properties are investigated by optical microscopy and electron backscatter diffraction (EBSD) in a scanning electron microscope. The analysis of the EBSD pattern demonstrates that the crystalline islands at intermediate stages of the re-crystallization process exhibit different orientations. We conclude that the re-crystallization process is driven by nucleation without any orientation information from the substrate. © 2012 American Institute of Physics. [<http://dx.doi.org/10.1063/1.4728221>]

I. INTRODUCTION

Phase-change materials (PCM) as exemplified by quasi-binary alloys in the $(\text{GeTe})(\text{Sb}_2\text{Te}_3)$ system, in particular $\text{Ge}_2\text{Sb}_2\text{Te}_5$, are very important materials for a variety of non-volatile memory devices such as rewritable digital versatile disks (DVD) commercialized by Matsushita in the 1990s and electrical phase-change random access memory (PCRAM), the latter of which is still under active development. The interest in PCRAM has recently intensified since it possesses much better scalability and switching speed than the currently used flash memory and may replace the latter in the near future.^{1,2} Furthermore, it may also supersede conventional dynamic random access memory (DRAM). This would result in a computer architecture, where operational and long-term information storage are consolidated in a single storage device.

The storage of information in PCM-based devices is achieved by optical or electrical switching between the metastable crystalline and the amorphous state. The stored data can be retrieved optically (DVD) by using the variation of the reflectance of about 30% or electrically (PCRAM) by utilizing the variation of the resistivity by several orders of magnitude between the crystallized and amorphized state.^{3–5} However, the details of the structural changes during the amorphization and re-crystallization process are still discussed controversially.

In the conventional picture of laser switching, the amorphization process occurs via supercooling after application of a short laser pulse that melts the material, while the re-crystallization process is performed using more gentle optical heating reaching the crystallization temperature. Recently, it has been shown that, in contrast to the current consensus, the crystal-to-amorphous transition may not involve conventional

melting, but may proceed through a photoexcited state that may trigger rupture of sacrificial (resonant) bonds leading to a collapse of the ordered phase.⁶

The re-crystallization process of sputter-deposited amorphous $\text{Ge}_2\text{Sb}_2\text{Te}_5$ films as determined via pulsed laser heating is dramatically retarded by about two orders of magnitude (from about 30 ns to about 3 μs), when nitrogen dopants are introduced.⁷ Time-resolved reflectivity measurements on $\text{Ge}_2\text{Sb}_2\text{Te}_5$ thin films have shown that the crystallization time is about 56 ns, while the amorphization time is about 3 ns.⁸ Very recently, the laser-induced crystallization and amorphization processes in $\text{Ge}_2\text{Sb}_2\text{Te}_5$ have been investigated using nanosecond-scale time-resolved diffraction with intense electron pulses.⁹ Using a unique and unconventional specimen geometry, cycling between the amorphous and crystalline phases was achieved, enabling *in-situ* transmission electron microscopy (TEM) studies of both microstructural and crystallographic changes caused by repeated switching. The crystallization time observed in their study amounts to about 2 μs . Note that these times can strongly depend on the film thickness, substrate, and pulse length of the laser used for the switching experiments.

We investigate epitaxial $(\text{GeTe})(\text{Sb}_2\text{Te}_3)$ films close to the $\text{Ge}_2\text{Sb}_2\text{Te}_5$ composition, where the change in the reflectance of the film between the metastable crystalline and the amorphous state can be as large as 30%.⁴ We combine optical switching experiments with structural information obtained from electron backscatter diffraction (EBSD) experiments in a scanning electron microscope. This allows for localized information of the crystallinity of the amorphized or re-crystallized film with a resolution of about 50 nm. In particular, the re-crystallization process, which is realized by applying a larger number of optical pulses with a much weaker intensity than for the amorphization process, is demonstrated to occur via many little steps, before the re-crystallized area exhibits the same crystal orientation as the as-grown $\text{Ge}_2\text{Sb}_2\text{Te}_5$ (GST) film.

^{a)}Electronic mail: flissi@pdi-berlin.de.

^{b)}Present address: Createc Fischer & Co. GmbH, Industriestr. 9, 74391 Erligheim, Germany.

II. EXPERIMENTAL DETAILS

The investigated GST film with a thickness of about 90 nm has been grown by molecular beam epitaxy (MBE) on a lattice-matched GaSb(001) substrate in order to guarantee a high structural quality. Due to the MBE growth and the selected growth parameters, the epitaxial film is completely crystalline directly after growth.^{5,10} Using reflection high-energy electron diffraction (RHEED), the investigated film was shown to exhibit a cubic crystal structure. GST films for commercial applications and most other scientific investigations are produced by sputter deposition and are usually amorphous directly after growth. Therefore, the sputtered films need to be heated to the crystallization temperature in order to become crystalline.

For our optical switching experiments, we use a high-power Nd:YAG laser (Continuum Leopard SV-20) operating at a wavelength of 532 nm, providing pulses of 60 ps duration with a maximum repetition rate of 20 Hz. Individual laser pulses can be extracted by a shutter system. The maximum energy for an individual laser pulse is 60 mJ. In order to select a specific value of the energy fluence, a set-up of several optical density filters and two adjustable polarizers are used. Since the energy per pulse is a critical parameter for the switching process, the energy of each laser pulse applied to the sample is measured using a beam splitter and a power meter. The laser-induced change of the reflectance of a specific area on the GST film is synchronously monitored by reflecting the light of a diode laser with a wavelength of 635 nm, which is detected using a photo-diode and lock-in technique. In order to investigate the crystal structure of the GST film before and after laser switching, EBSD measurements are performed. The EBSD system (EDAX DigiView IV EBSD Detector) is attached to a scanning electron microscope (SEM, Zeiss ULTRA 55), and a sophisticated software (EDAX OIM V5.3) is used to analyze the EBSD patterns. In order to prevent oxidation of the GST film, it is mounted in a vacuum chamber during storage and laser switching. All presented measurements have been recorded at room temperature.

III. RESULTS AND DISCUSSIONS

Figures 1(a) and 1(b) display an exemplary time dependence of the normalized reflectance R/R_c , where R_c denotes the measured reflectance of the crystalline phase, and the corresponding energy fluence ρ_E of the applied laser pulses, respectively, for a complete switching cycle. Between $t = 7$ and 28 s, ten laser pulses are applied separated on the average by $\tau_p = 2.3$ s. The stepwise reduction of R/R_c demonstrates that the amorphization process (AP) takes place discretely, where each laser pulse contributes separately. For the AP, an average value of $\rho_E \approx 17$ mJ/cm² was used so that the sample was only partly amorphized in the exposed area resulting in a minimal achievable normalized reflectance R_{\min}/R_c of about 0.9. Note that there is a minimum energy fluence necessary for the AP to occur, which also depends on the crystallization state of the film. If ρ_E is below that value, a re-crystallization process (RCP), i.e., an increase in R/R_c , may take place instead of an AP. After

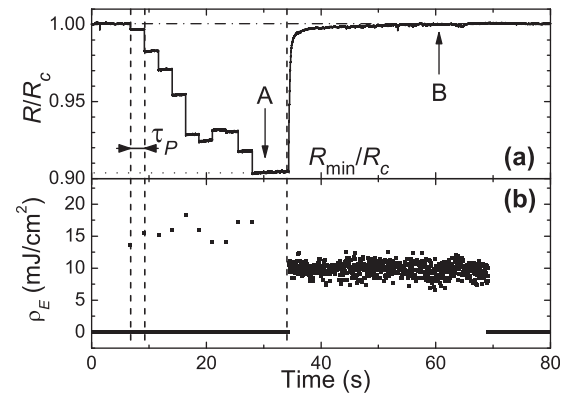


FIG. 1. (a) Normalized reflectance R/R_c vs. time during a complete switching cycle with a time resolution of 2.5 ms. The labels A and B refer to the amorphized and re-crystallized state, respectively. τ_p denotes the laser pulse separation and R_{\min}/R_c the minimal achievable normalized reflectance using this particular energy fluence for this AP. (b) Energy fluence ρ_E of the applied laser pulses vs. time.

$t = 34$ s, a chain of laser pulses with a lower value of ρ_E and a pulse separation of 50 ms was applied. The RCP manifests itself by the recovery of R to almost its original value R_c .

The different refractive indices of the GST film after an AP [label A in Fig. 1(a)] and a RCP [label B in Fig. 1(a)] result in a strong contrast of optical-microscope images as depicted in Figs. 2(a) and 2(b), respectively. In order to demonstrate that the exposed area in Fig. 2(a) is amorphous and in Fig. 2(b) crystalline, we recorded EBSD patterns for representative spots in both areas as shown in Figs. 2(c) and 2(d), respectively. While the area after a RCP in Fig. 2(d) clearly shows the presence of Kikuchi lines indicative of a crystalline structure (backscattered electrons are diffracted

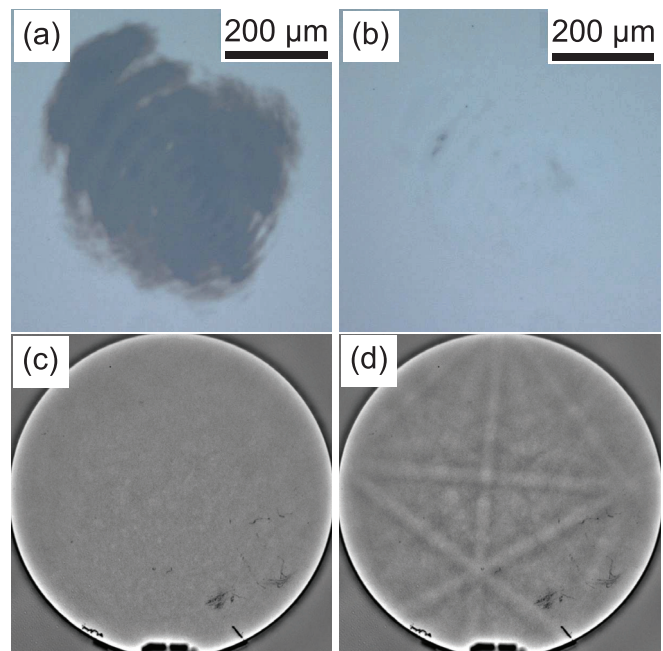


FIG. 2. Optical-microscope images of two areas on the sample surface after (a) a complete amorphization [comparable to label A in Fig. 1(a)] and (b) a complete re-crystallization process [comparable to label B in Fig. 1(a)]. (c) and (d) EBSD patterns recorded for a representative spot inside the areas in (a) and (b), respectively.

by the crystal structure of the GST film), these lines are completely absent for the amorphized area in Fig. 2(c). Therefore, we can conclude that the area after an AP is amorphous. The indexing of the Kikuchi lines in Fig. 2(d) reveals a cubic crystal structure with (001) orientation. The effective depth of penetration of the electron beam into the film is of the order of 20–30 nm so that, after an AP or a RCP, the GST film is switched over at least one third of the film thickness between the amorphous and crystalline state.

The AP depends strongly on the selected value of ρ_E . In Fig. 3, the smallest achievable values of the normalized reflectance R_{\min}/R_c for switching cycles with different values of ρ_E are displayed. For $\rho_E < 12 \text{ mJ/cm}^2$, the reflectance did not change so that no AP took place. For $12 \text{ mJ/cm}^2 < \rho_E < 25 \text{ mJ/cm}^2$, the reflectance is clearly reduced so that amorphization has occurred, but several laser pulses are necessary to reach R_{\min}/R_c . If additional laser pulses are applied, the reflectance value does not change anymore. For $\rho_E > 25 \text{ mJ/cm}^2$, a single laser pulse was usually sufficient to reach R_{\min}/R_c , which in this range of ρ_E values is more or less independent of the exact value of ρ_E . For $\rho_E > 35 \text{ mJ/cm}^2$, the GST film was damaged, which implies that a complete RCP is not possible anymore. We identify the saturation value of $R_{\min}/R_c = 0.69$ at $\rho_E > 25 \text{ mJ/cm}^2$ as the normalized reflectance R_a/R_c of an amorphous GST film.

For the re-crystallization process, the normalized reflectance is displayed in Fig. 4 for a value of ρ_E of 15 mJ/cm^2 over a time window of 0.5 s, which corresponds to a small part of the time window shown in Fig. 1, for two different laser pulse separations. This measurement clearly shows that R increases in a step-like way for each applied laser pulse. The width of the steps corresponds to the separation of the laser pulses. We conclude that this chain of RCP pulses does not generate an average temperature increase above the crystallization temperature. Therefore, the GST film does not crystallize continuously but in multiple steps.

In order to investigate the RCP in more detail, three different areas on the GST film were first amorphized. Subsequently, the RCP was interrupted at different points in time.

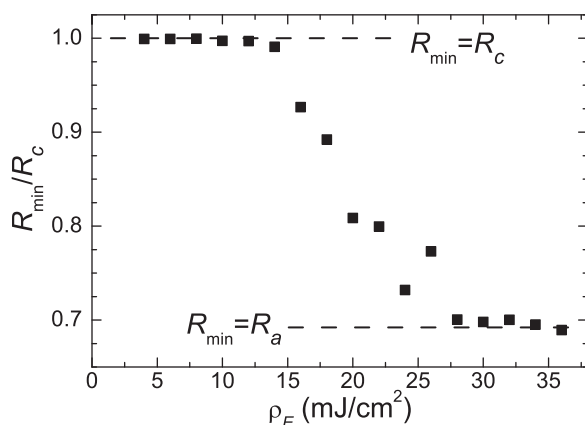


FIG. 3. Smallest achievable value of the normalized reflectance R_{\min}/R_c during an AP as a function of ρ_E for a particular area with a diameter of approximately $300 \mu\text{m}$. For each value of ρ_E , a different number of amorphization pulses was applied, until the reflectance reached a constant value.

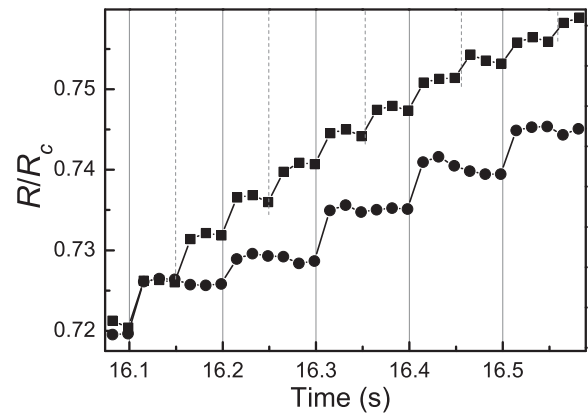


FIG. 4. Normalized reflectance vs. time with a time resolution of 16.6 ms during the beginning of the RCP with a value of ρ_E of 15 mJ/cm^2 for laser pulse separations of 50 (squares) and 100 ms (dots). The vertical dashed and solid lines indicate the point in time, when the laser pulse was applied.

In Figs. 5(a)–5(c), three optical-microscope images are displayed showing three areas, where the RCP was terminated shortly after its beginning, after nearly 50% of the initial reflectance value R_c was recovered, and close to the value of R_c , respectively. In all three images, small islands are clearly visible. Note that the large islands on the scale of several tens of micrometers are due to interference fringes of the laser inside the exposed area. With more and more laser pulses of the RCP, more and more islands appear, which finally form a connected area. The small islands have always nearly the same size. The fact that the RCP takes place by generating more and more such islands, which themselves do not grow, is an indication for the fact that the RCP is

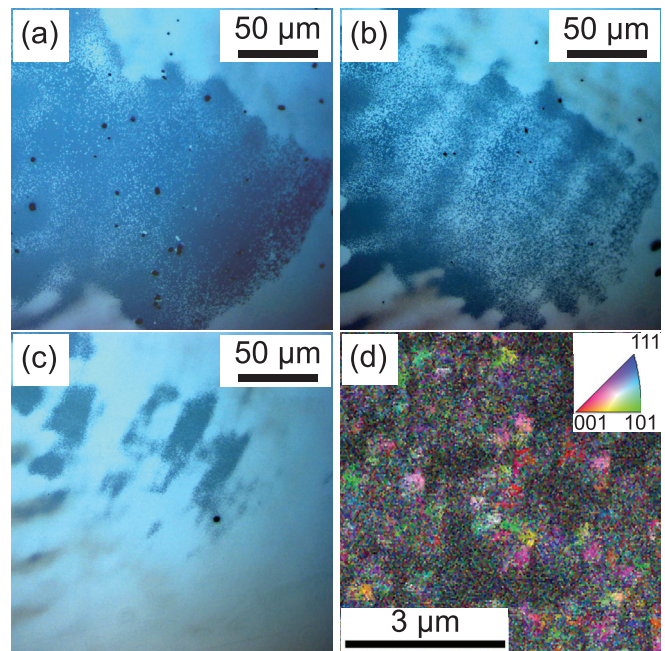


FIG. 5. (a)–(c) Optical-microscope images of the GST film for different stages of the re-crystallization process, the RCP was terminated (a) shortly after its beginning, (b) after nearly 50% of the initial reflectance value R_c was recovered, and (c) close to the value of R_c . (d) EBSD out-of-plane orientation map recorded within the partially re-crystallized area shown in (b) indicating the presence of small crystalline islands with different orientations on an amorphous background.

driven by nucleation and not by growing from the crystalline edges of the amorphous area. Figure 5(d) shows a color-coded EBSD out-of-plane orientation map. The color code [see inset of Fig. 5(d)] indicates different crystal orientations on the basis of an inverse pole figure. Amorphous areas are indicated by black pixels corresponding to a low contrast of the EBSD pattern. The small crystalline islands can be clearly identified by the small clouds with different colors. Each of these clouds has a different crystal orientation. This random orientation suggests that the island did not receive any orientation information from the substrate, which could be an indication for the fact that the nucleation takes place in the topmost part of the GST film. EBSD measurements on an area where the RCP is completed reveal that the GST film is homogeneously oriented and exhibits the same orientation as directly after growth.

The above findings, i.e., that the AP and RCP take place in steps and that the number of steps as well as R_{\min} can be selected by the appropriate value of ρ_E , suggest that on a single area multiple bits can be stored. Usually, a modulation of ρ_E (optical switching) or of the heater current (electrical switching) is necessary to achieve different states of crystallization. In the scenario presented here, only two values of ρ_E , one for RCP (set) and one for AP (reset), are necessary, while the level of crystallization which encodes the different bits is defined by the number of applied switching pulses. Since only two current values have to be controlled in this case, the control electronics can be significantly simplified. Note that, under these conditions, such a memory cell should have a diameter of several micrometers, because it has to consist of more than one crystallization island. The diameter of one crystallization island can be estimated from Fig. 5(d) to be slightly below 1 μm .

IV. CONCLUSIONS

We optically switched GST films with laser pulses of 60 ps duration for different energy fluences. Depending on the

selected value of ρ_E , the amorphization process can take place in a single or in multiple steps. In contrast, the re-crystallization process always takes place in multiple steps. Intermediate stages of the re-crystallization process are characterized by small crystalline islands within the amorphous area. The crystallinity of these islands was verified by EBSD, which also demonstrates that the islands exhibit different orientations. These observations suggest that the re-crystallization process is driven by nucleation without any orientation information from the substrate. After the re-crystallization process is completed, EBSD measurements reveal that the whole re-crystallized area exhibits the same crystal orientation as the as-grown GST film.

ACKNOWLEDGMENTS

The authors acknowledge fruitful discussion with R. Calarco and P. Rodenbach. Partial financial support is gratefully acknowledged through funding by the Deutsche Forschungsgemeinschaft.

¹M. Wuttig, *Nature Mater.* **4**, 265 (2005).

²G. I. Meijer, *Science* **319**, 1625 (2008).

³S. Privitera, C. Bongiorno, E. Rimini, and R. Zonca, *Appl. Phys. Lett.* **84**, 4448 (2004).

⁴W. Welnic and M. Wuttig, *Mater. Today* **11**, 20 (2008).

⁵W. Braun, R. Shayduk, T. Flissikowski, M. Ramsteiner, H. T. Grahn, H. Riechert, P. Fons, and A. Kolobov, *Appl. Phys. Lett.* **94**, 041902 (2009).

⁶P. Fons, H. Osawa, A. V. Kolobov, T. Fukaya, M. Suzuki, T. Uruga, N. Kawamura, H. Tanida, and J. Tominaga, *Phys. Rev. B* **82**, 041203(R) (2010).

⁷R. M. Shelby and S. Raoux, *J. Appl. Phys.* **105**, 104902 (2009).

⁸H. Huang, F. Zuo, F. Zhai, Y. Wang, T. Lai, Y. Wu, and F. Gan, *J. Appl. Phys.* **106**, 063501 (2009).

⁹M. K. Santala, B. W. Reed, T. Topuria, S. Raoux, S. Meister, Y. Cui, T. LaGrange, G. H. Campbell, and N. D. Browning, *J. Appl. Phys.* **111**, 024309 (2012).

¹⁰W. Braun, R. Shayduk, T. Flissikowski, H. T. Grahn, H. Riechert, P. Fons, and A. Kolobov, *Materials and Physics for Nonvolatile Memories*, *Mater. Res. Soc. Proc.* Vol. 1160, edited by Y. Fujisaki, R. Waser, T. Li, and C. Bonafos (MRS, Pittsburgh, 2009), p. H14–05.